

The Ages of M31 Star Clusters: Spectral Energy Distribution Versus Color-Magnitude Diagram

Zhou Fan¹, Zhongmu Li², Gang Zhao^{1,3}

zfan@bao.ac.cn

ABSTRACT

It is well-known that fitting the Color Magnitude Diagrams (CMDs) to the theoretical isochrones is the main method to determine star cluster ages. However, when the CMDs are not available, the Spectral Energy Distribution (SED)-fitting technique is the only other approach, although it suffers the age-metallicity-reddening degeneracy. In this work, we gather the ages, metallicities and masses of dozens of M31 star clusters from the CMD-fitting with HST images from the literatures for comparison. We check the reliability of the SED-fitting results with different models, i.e., Bruzual & Charlot 2003 model (BC03), Galaxy Evolutionary Synthesis Models (*GALEV*) and Advanced Stellar Population Synthesis (ASPS) for the simple stellar populations (SSPs) with single stars (ss)-SSP/binary star (bs)-SSPs models. The photometry bands includes the Galaxy Evolution Explorer *GALEX* FUV/NUV bands, optical/near-infrared *UBVRIJHK* bands, as well as the Wide-field Infrared Survey Explorer (*WISE*) *W1/W2* bands. The comparisons show that the SED-fitting ages agree well with the CMD-fitting ages, either with the fixed metallicity or with the free metallicity for both the BC03 and the *GALEV* model. However, for the ASPS models, it seems that SED-fitting results are systematic older than the CMD ages, especially for the ages $\log t < 9.0$ (yr). The fitting also shows that the *GALEX* FUV/NUV-band are more important than the *WISE* *W1/W2* for constraining the ages, which confirms the previous findings. We also derived the masses of our sample star clusters from the BC03 and *GALEV* models and it is found that the values agree well with that in the literature.

¹Key Laboratory of Optical Astronomy, National Astronomical Observatories, Chinese Academy of Sciences, Beijing 100101, China

²Dali College, Dali, Yunan 671000, China

³School of Astronomy and Space Science, University of Chinese Academy of Sciences, Beijing 100049, China

Subject headings: galaxies: individual (M31) — galaxies: star clusters — globular clusters: general — star clusters: general

1. Introduction

Stellar population fitting techniques are important to determine the physical parameters (e.g., ages, metallicities, and masses) for the spatially unresolved stellar population. The CMD-fitting is the main approach to limit the age of star clusters. It is reliable as the stars of a cluster distribute on an isochrone if they have the same metallicity and age. Because M31 is close enough to the Milky Way, the CMDs of M31 star clusters can be observed well via the Hubble Space Telescope (HST) and some large ground-based telescopes (Rich et al. 2005). This makes us able to study these clusters using CMDs. For instance, Perina et al. (2009a) observed the star cluster VdB0 with the Wide Field and Planetary Camera 2 (WFPC2) on the HST and fit the observed CMD with the isochrone, giving the age, metallicity and mass estimates. Perina et al. (2009b) analyzed the number of M31 globular clusters (GCs) with reliable CMDs, and found that the number of young and old GCs are 11 and 44, making use of the CMD structure features. Perina et al. (2010) obtained the ages and masses estimates of 19 clusters in M31 with the WFPC2 on HST data by fitting the CMD and the theoretical isochrones. A sample of 24 star clusters with CMD-fitting ages have been gathered. In addition, Perina et al. (2011) present deep *BV* photometry for four intermediate-age (1-9 Gyrs) M31 GCs with the wide field channel of the Advanced Camera for Surveys (ACS) on board *HST* and test how the age estimates from integrated spectroscopy or photometry can be supported by CMD-fitting. The authors also give the minimum ages of three M31 star clusters by fitting the isochrone and upper main sequence (MS) stars and sub-giant branch (SGB) stars of CMD. Williams & Hodge (2001) also determined the age of four M31 star clusters by the isochrone fitting by eye and the software package MATCH, and it is found that the ages from the two methods are in good agreement. We are showed that only the ages of a part of clusters can be estimated similarly by different methods. Such works can be completed using some classical stellar population models, e.g., BC03 (Bruzual & Charlot 2003) and ASPS (Li & Han 2008; Li et al. 2012, 2017). For the study of CMDs with different stellar population models one may see the papers (e.g., Li et al. 2015, 2017; Li & Deng 2018; Luo & Li 2018).

However, in some case, there is an age difference between SED and CMD fitting determinations, which is possibly caused by various constraints used in studies. In detail, the CMD ages are determined mainly by comparing the observed turn-off point to that of

theoretical isochrones using an eye-aided method, when taking fixed distance and reddening (Perina et al. 2009a, 2010, 2011). This kind of isochrone-fit result is affected by IMF slightly, but it is not the case of SED fitting. In order to compare SED and CMD fitting determinations, both the CMD and luminosity function should be fitted, because luminosity function is also sensitive to IMF. It should be noted that there are obvious uncertainties in age determinations, even in CMD fitting. In the cases of some CMD parts or luminosity functions not fitted well, there will be large uncertainties in the CMD ages, which can contribute to the age difference. For instance, overshooting and stellar binarity can affect the result obviously. The age difference between CMD fitted ages from models can be as large as a factor of 0.6 (Perina et al. 2009a). In addition, the use of different isochrones (considering the overshooting or not) also contributes to the age difference, which may lead to SED fitted ages younger than ~ 0.4 dex compared to CMD fitted ages.

The χ^2_{\min} SED-fitting of globular clusters is an efficient method to determine the parameters on the basis of multi-passband photometry/imaging data when the CMDs are not available. Previously, de Grijs et al. (2003) derive the ages, metallicities, and reddening of the star clusters associated with NGC 3310 by the SED-fitting method with the photometry of the ultraviolet (UV), optical, and near-infrared (NIR) observations obtained with the *Hubble Space Telescope* (*HST*). Fan et al. (2006); Ma et al. (2007, 2009, 2011, 2012); Wang et al. (2010, 2012) have done a series of SED-fitting works of M31 star clusters, based on the Beijing–Arizona–Taiwan–Connecticut (BATC) multi-color photometry system, with a 60/90cm Schmidt telescope. The simple stellar population (SSP) models applied are the Bruzual & Charlot (2003, henceforth BC03) and the Galaxy Evolutionary Synthesis Models (*GALEX*; Lilly & Fritze-v. Alvensleben 2006; Kotulla et al. 2009). To achieve better results, the photometry on their bands, such as the broad-band *UBVRI* filters, the Two Micron All Sky Survey (2MASS) *JHK* bands, the Galaxy Evolution Explorer (*GALEX*) near-UV (NUV) and far-UV (FUV) channels, as well as the Sloan Digital Sky Survey (SDSS) *ugriz* bands have been applied. With considering the contributions of binary merger products in the form of blue straggler stars Fan & de Grijs (2012) also fitted the SEDs in *UBVRIJHK* and *ugriz* bands of M31 globular-like clusters with the models including the bs-SSPs model. Since the Wide-Field Infrared Survey Explorer (*WISE*; Wright et al. 2010) provides mid-infrared (mid-IR) *W1/W2*-band data, of which the limiting magnitude could match the SED of M31 star clusters, we also extend the wavelength range of SED to these bands.

In our work, we derived the ages and metallicities of our sample M31 star clusters with SED-fitting based on the photometry bands from the *GALEX* FUV/NUV bands to the broadband *UBVRI* bands and NIR *JHK* and *WISE W1/W2* bands. All the sample star clusters already have the ages and metallicities fitted with the CMDs in the literature. Thus we compared our results of the SED-fitting and that from the CMD-fitting results in

the literatures. The organization of the paper is as follows. In Section 2 we introduce the models mainly applied and convolutions of the passbands. In Section 3, we describe the selection of sample and introduce the methods adopted for the fits. In Section 4 we provide the best-fitting results as well as comparisons of the ages and masses based on χ^2_{\min} fitting with various models. Finally, the summary, concluding remarks and the future works are given in Section 5.

2. The Models and the χ^2_{\min} -fitting Method

The BC03 synthesis models (Bruzual & Charlot 2003) is one of the most commonly-used models for the SSP fitting, which could provides the spectra and SEDs for different parameters, e.g., age, metallicity. The models includes the 1994 and 2000 Padova stellar evolutionary tracks as well as the stellar initial mass functions (IMFs) of Salpeter (1955) and Chabrier (2003) and the wavelength coverage is 91 Å-160μm. The models includes six metallicity values ($Z = 0.0001, 0.0004, 0.004, 0.008, 0.02, \text{ and } 0.05$) for Padova 1994 tracks, while another six metallicities ($Z = 0.0004, 0.001, 0.004, 0.008, 0.019, \text{ and } 0.03$) are included for the Padova 2000 tracks. For the age, there are 221 values 0-20 Gyr in unequally spaced time steps could be used. In our work, the upper limit of age is set to 13.8 Gyr, which is Planck’s latest estimate of age of the universe (Ade et al. 2016). In order to reduce the intervals of metallicity space and obtain better results which seems “more accurate” or “higher resolution” as the grids of metallicity space are smaller in the models and thus closer to the nearest SSP in our fitting, we interpolate the original metallicities the models to 51 metallicities with equal steps in logarithmic space rather than the original only six values. Since the Chabrier (2003) IMF and Padova 2000 track are more up-to-date, they have been adopted in our fits and comparisons.

The *GALEV* models (Kotulla et al. 2009) are also commonly used to explore the abundance evolution of gas and the spectral evolution of the stellar populations, e.g., star clusters or galaxies. It provides the stellar evolutionary tracks and isochrones from the Padova and Geneva groups. In this work, Padova evolutionary tracks are adopted. The simple stellar populations (SSPs) models provide 5001 ages 4 Myr16 Gyr and 7 metallicities ($Z = 0.0001, 0.0004, 0.001, 0.004, 0.008, 0.02, \text{ and } 0.05$). The upper limit of age is also set to age of the universe 13.8 Gyr from the new result of Planck as done in BC03 model for the reason of comparisons. Since the number of metallicity values in the model are not enough for the fit, we interpolate the metallicities to a grid of 51 values as done previously, which can yield better results than the basic model set. The model spectra are in the wavelength coverage 90 Å-160 μm, which is, convenient for us to convolve the model spectra with the filter trans-

mission curves and obtain the model magnitudes. There are two commonly-used options for the IMF: Salpeter (1955) and Kroupa (2001). Thus, in our work, Kroupa (2001) IMF is adopted for the fitting as it is more up-to-date and more reasonable than the Salpeter (1955) for the *GALEV* model.

The ASPS models which built both single-star simple stellar populations (ss-SSPs) and the binary-star simple stellar populations (bs-SSPs) models (Li et al. 2012, 2016) is developed from the rapid population synthesis (RPS) model (Li & Han 2008). The main feature of ASPS models is that it takes into account single stars, binary stars and rotating stars, simultaneously. Thus different stellar population models including classical ss-SSPs and bs-SSPs can be used to study star clusters. In ASPS models, some typical parameter distributions (e.g., orbital eccentricity and mass ratio) and widely used IMFs (e.g., Salpeter 1955) are used for the stars of a population and the rapid stellar evolutionary code of Hurley et al. (2000, 2002) is used for computing stellar evolution. The effect of rotation on stellar evolution is also considered using some recent results (e.g., Georgy et al. 2013). For the standard models, eight metallicities ($Z = 0.0001, 0.0003, 0.001, 0.004, 0.008, 0.01, 0.02$ and 0.03) and 151 ages (0-15 Gyr with an interval of 0.1 Gyr) have been taken. The fractions of binary stars and rotating stars can change from zero to 1.

For BC03 SSP models, *GALEV* models and the ASPS ss-SSPs/bs-SSPs models, the theoretical spectra have been convolved into the AB system with the transmission of filters in the FUV, NUV, *UBVR IJHK*, *W1*, and *W2* bands (Jarrett et al. 2011). The AB magnitudes of the models are calculated in the formula (see, e.g., Fan et al. 2006; Ma et al. 2007, 2009, 2011, 2012; Wang et al. 2010, 2012) below,

$$m_{\text{AB}}(t) = -2.5 \log \frac{\int_{\lambda_1}^{\lambda_2} d\lambda \lambda F_{\lambda}(\lambda, t) R(\lambda)}{\int_{\lambda_1}^{\lambda_2} d\lambda \lambda R(\lambda)} - 48.60, \quad (1)$$

in the formula, $R(\lambda)$ is the transmission of the filters and $F_{\lambda}(\lambda, t)$ is the theoretical model flux, which is a function of wavelength (λ) and evolutionary time (t); λ_1 and λ_2 are the short- and long-wavelength cut-offs of the respective filters.

3. Cluster Sample Selection and χ^2_{min} Fitting

In order to compare the ages and mass estimates from CMD-fitting and that from the SED-fitting, we gather a sample which have the CMD-fitting from *HST* observations previously. The GCs of Our sample are from the master catalog of Perina et al. (2010) and Perina et al. (2011). Perina et al. (2010) estimated the ages and metallicities of 19 star clusters with the CMD-fitting method. The data is from HST/WFPC2 survey of the bright

young star clusters of M31. In order to analyze, the ages and metallicities of six star clusters from Perina et al. (2009b) and four clusters from Williams & Hodge (2001) also included. Perina et al. (2009b) used the HST/ACS archive data and the solar abundance isochrone of Girardi et al. (2002) while Williams & Hodge (2001) used observational data from WFPC2 imager aboard the HST and the isochrone of Bertelli et al. (1994). Thus the master catalog includes 29 GCs. In addition, Perina et al. (2011) gives the lower limits of ages for three star clusters, B292, B337 and B350 by fitting the isochrones with the observed CMDs, especially for the SGB stars. Our final sample consists of 32 star clusters with ages and metallicities already derived using the CMD fitting technique.

We collected photometry of M31 star clusters and candidates from the UV to the mid-IR. The *GALEX* FUV/NUV data, the *UBVRI* broad-band data and the 2MASS *JHK* data were obtained from the Revised Bologna Catalog of M31 globular clusters and candidates⁴ (RBC v.5; Galleti et al. 2004, 2006, 2009). The data consists of combined photometric observations, including the most updated ones. The FUV/NUV-band photometry are actually from RBC v.5, which is composed of data of Rey et al. (2007); Kang et al. (2012). The *UBVRI*-band photometry are from RBC v.5, which is composed of optical photometry of dozens of various works, including the updated works, (e.g., Fan et al. 2010; Peacock et al. 2010). For the *JHK*-band photometry, although RBC v.5 provides the photometry mainly from Galleti et al. (2004), Perina et al. (2010) also give the aperture photometry of the $r = 10''.0$ from 2MASS-6X-PSC catalog. In our work, we merge the two catalogues and the photometry with smaller errors is adopted if both RBC and Perina et al. (2010) have the available *JHK*-band photometry. In fact most of the photometry is adopted from Galleti et al. (2004), which is more precise. For the *WISE* photometry: the central wavelengths of *W1*, *W2*, *W3*, and *W4* bands are 3.4, 4.6, 12 and 22 μm . The limiting magnitudes (adopting a signal-to-noise ratio of 5 for 11-frame composite images) are 17.11, 15.66, 11.40, and 7.97 mag (Wright et al. 2010). Since the limiting magnitude of the *W3* and *W4* bands are not sufficiently high for our analysis. The photometry and associated uncertainties of *WISE W1* and *W2* bands (in the Vega system), is in fact from the work of Fan & Wang (2017). For the BC03/*GALEX* model fit, we use bands *GALEX* FUV/NUV, *UBVRIHJK*, *WISE W1/W2* magnitude currently. Thus we only have 12 bands for the SED-fitting.

In order to fit the multi-band photometry based on the convolved SED models discussed in Section 2, we then converted all Vega-based photometry to the AB system using the Kurucz (1992) SEDs of Vega, which could be used to be convolved with the filter transmission to obtain the system offset between the Vega magnitude and AB magnitude. The SED of

⁴<http://www.bo.astro.it/M31/>

Vega is well-studied, thus the errors of the system offset is too small to be considered, compared to the observational errors and model errors. We fit the SEDs of the observational magnitude and model magnitude, which should be in the same system, either in AB or Vega. Here we use the AB system for the SED-fitting, thus all the magnitudes are converted to the AB system except the FUV/NUV as they have been in AB system previously. Since this process only changes the offset of two systems, it dose not affect errors, e.g., $\sigma_{M,i}$ in equation 2, at all.

Since the reddening affects SED fitting seriously, we adopted reddening values for our sample star clusters from Table 2 of Perina et al. (2010), which is also a combination of the values from their own work and those from literature. A_λ is estimated with equations of Cardelli et al. (1989), and a typical foreground Milky Way extinction law, $R_V = 3.1$ is adopted. SEDs are fitted by using the equation following,

$$\chi^2_{\min} = \min \left[\sum_{i=1}^{12} \left(\frac{M_{\lambda_i}^{\text{obs}} - M_{\lambda_i}^{\text{mod}}(t, [Z/H])}{\sigma_{M,i}} \right)^2 \right], \quad (2)$$

where $M_{\lambda_j}^{\text{mod}}(t, [Z/H])$ is the i^{th} model magnitudes with age t and metallicity $[Z/H]$, while $M_{\lambda_i}^{\text{obs}}$ is the observed, reddening-corrected magnitude in the i^{th} band.

For the ASPS model fit, we use only the band *GALEX* FUV/NUV, *UBVRIHJK* as the model dose not provide the *WISE* *W1/W2* band magnitude currently. Thus the Equation 2 is applied using only ten photometric bands.

For the uncertainty estimate in the fits, we use the Equation (3),

$$\sigma_{M,i}^2 = \sigma_{\text{obs},M,i}^2 + \sigma_{\text{mod},M,i}^2, \quad (3)$$

where $\sigma_{M,i}$ represents the total magnitude uncertainty in the i^{th} band. The photometric uncertainties in the RBC v.5 magnitudes are estimated as Fan et al. (2016), i.e., 0.08 mag in *U* band, 0.05 mag in *BVRI* bands, 0.1 mag in *J* band, and 0.2 mag in *HK* bands (Galleti et al. 2004). The photometric errors in the *GALEX* filters are provided in the RBC; for the *W1/W2* bands, the uncertainties are included in Table 1 of Fan & Wang (2017). For the model uncertainties, we adopted the typical error 0.05 mag for BC03 and *GALEV* SSP models, as done previously by Fan et al. (2006); Ma et al. (2007, 2009); Wang et al. (2010); Fan & de Grijs (2014).

For the comparison, we also did the SED-fitting with the fixed metallicity from the Perina et al. (2010, 2011) with the three models. The fitting results are listed in the Tables 1–6.

4. Fit Results and Discussion

To check the results from the SED-fitting, we compared with the resulting ages from CMD-fitting from various sources in the literature. Figure 1 shows the cluster ages as derived from SED-fitting with Padova 2000 evolutionary tracks and a Chabrier (2003) IMF, adopting BC03 models, compared with age determinations from the CMD-fitting of Perina et al. (2010, 2011) in y-axis. In the left panel, ages in our work are derived from SED-fitting with free-metallicity in the BC03 models. It is found that the agreement is good overall except for a few outliers for the older ones ($\log t > \sim 10$) (yr). In the right panel, ages from our estimates are derived with fixed metallicities, which are actually from the CMD-fitting of literature Perina et al. (2010, 2011). It is found that ages from free-metallicity is also consistent with the CMD results, which is the same as that in the left panel. For the old part ($\log t > \sim 10$) (yr), the agreement seems slightly better than the left panel. The comparison implies that the SED-fitting is reliable and reasonable for the age fittings.

To estimate the effects of using the *GALEX* FUV/NUV bands in the SED-fitting, we have done the same comparison in Figure 2 as in Figure 1, but without the *GALEX* FUV/NUV bands. It can be seen that the results are much worse than that in Figure 1, especially for the young clusters ($\log t < 8.5$ yr). The mean error increase from 0.22/0.24 dex to 0.41/0.40 dex in logarithmic space for the free-metallicity/fixed-metallicity fitting, compared to Figure 1. The same comparison is done in Figure 3 to estimate the effect of the WISE *W1/W2* bands. However, it seems that the results do not change much as that in Figure 1, indicating that the WISE *W1/W2* bands do not effect significantly, compared to that of the *GALEX* FUV/NUV bands. It confirms the conclusions of Fan & Wang (2017), i.e., the *GALEX* FUV/NUV bands effect much more significantly in the SED-fittings than the other bands, especially for the WISE *W1/W2* bands. It is known that the integrated colours technique is affected by the effects of stochastic sampling of the IMF, while this could not be the case for CMD ages if they are derived from the best fitting isochrone, for example. Thus it is important to address the differences between the two different methods. It is discussed the stochastic fluctuations effect increases the uncertainties of predicted colours and magnitudes associated with the resulting model parameters, particularly for the lower mass clusters $\leq 1 \times 10^4 M_{\odot}$ (Bruzual 2010; Fan & de Grijs 2012; Anders et al. 2013). In our work, the fraction for the less massive clusters ($\leq 10^4 M_{\odot}$) is 5/28 (from P10/P11) or 8/32 (for BC03 model with free-metallicity fitting) or 7/32 (for *GALEX* model with free-metallicity fitting), which are small fraction. In fact the fraction is even less if we rule out the clusters whose mass are significant much smaller than $\leq 10^4 M_{\odot}$. Thus we think the stochastic sampling effect is insignificant in our SED-fitting.

In order to check the effect of different models, we also fit with other models. Figure 4

is the same as Figure 1 but for the *GALEV* models with a Kroupa (2001) IMF. Similarly, we compare the best-fitting SED resulting ages with free-metallicity are shown in the left panel and those with fixed metallicity are shown in the right panel. It can be seen that the fitting results are systematically younger than the CMD-fitting results for the older clusters, i.e., ($\log t > 9.5$ yr), although for the younger clusters the agreement is well. This could be due to the model difference, which has been mentioned by many previous works, e.g., Fan & de Grijs (2012).

Figures 5–6 are the same as Figure 1 but for the ASPS ss-SSPs/bs-SSPs models without WISE W1/W2 band photometry, as it is not included in the the models. We note the presence of systematic differences in both left panel (metallicity-free fitting) and in the right panel (metallicity-fixed fitting), in both of the ss-SSPs (in Figure 5) and bs-SSPs models (in Figure 6). We see that for the ASPS ss-SSPs models/bs-SSPs models, SED-fitting results are systematic older than the CMD ages (~ 0.7 dex), especially for the ages $\log t < 9.0$ (yr). It may be due to the calibration of the models, as there is no such bias for the CMD-fitting and the SED-fitting with *GALEV* and BC03 models. It suggests that there may be a problem with the adopted stellar evolution models (independent from the inclusion of binaries). In the previous studies, Salpeter (1955) and Kroupa (2001) IMFs were used and the RSG star distribution was used to constrain stellar metallicity. As we see, the luminosity functions of many sample clusters were not fitted well, in particular for the bright end (e.g. B015D, B066, B040, B043 and B448). Some clusters are lack of reliable luminosity functions (B475 and V031) and their CMD ages were only from isochrone fitting, while some other clusters have no clear main sequences (e.g. B374, B222, B083, NB16 and B347) and only lower limits were given for their ages. This should contribute to the age difference between CMD and SED determinations.

In CMD fittings, a BASTI isochrone database was used, which has taken into account overshooting⁵. However, in the SED fittings, in particular ASPS fitting, overshooting usually was not considered. This may lead to some difference between SED and CMD fitted ages. If in SED fitting the age change caused by overshooting is similar to the case of CMD fitting (~ 0.4 dex) , it can roughly explain why the ages derived from ASPS models defer from CMD ages by 0.4–0.5 dex systematically. This effect is the same in both ss-SSP and bs-SSP models, so that we conclude that it is not due to the inclusion of binary stars. This effect is the same in both ss-SSP and bs-SSP models, so that we conclude that it is not due to the inclusion of binary stars.

The masses of M31 star clusters are also important physical parameters. Firstly, we

⁵<http://www.oa-teramo.inaf.it/BASTI/index.php>

would like to briefly define the different ways in which the masses are obtained:

- i. The masses calculated from the V_0 magnitude of Table 2 of Perina et al. (2010) and Perina et al. (2011).
- ii. The values from the literatures: the masses provided by Table 2 of Perina et al. (2010), which includes the results from Perina et al. (2009b), Williams & Hodge (2001) and their own work, and Perina et al. (2011).
- iii. The masses estimated from the SED-fitting directly in our work.

Previously, Perina et al. (2010) compute the masses of star clusters by using the dereddened absolute V_0 magnitude, which are from RBC.

Since BC03 models provide the mass-to-light ratio in V -band for the given age and metallicity in their models, the masses can be derived with the fitted parameters. In our work, the V -band magnitude are from the updated version RBC v.5, which includes the updated photometry from Fan et al. (2010); Peacock et al. (2010). The distance module $(m - M)_0 = 24.47$ (McConnachie et al. 2005) is adopted for the calculation of the absolute magnitude. The extinction values are from the literatures (e.g., Perina et al. 2010, 2011) and the extinction law is from Cardelli et al. (1989). The comparison of our SED-fitting results (iii) and that from literature (ii) is shown in figure 7. The top panels are the masses estimated with the free-metallicity SED-fitting results. In the left panel we use V_0 magnitudes from our work (iii) while in the right panel we adopt V_0 intrinsic magnitude from Table 2 of Perina et al. (2010) and Perina et al. (2011) (i). It can be seen that the agreement is good for our estimates (left panel, iii) and even better if the V_0 magnitude of Perina et al. (2010, 2011) are adopted (right panel, i). The bottom panels are the fixed-metallicity SED-fitting results (iii). Similarly, the mass estimates with intrinsic V_0 magnitude from Table 2 of Perina et al. (2010) and Perina et al. (2011) (i) agrees with the the mass estimates of literature (ii) much better than that with the V_0 magnitude in our SED-fitting (iii). This is mainly due to the different V_0 magnitudes of Table 2 of Perina et al. (2010) and Perina et al. (2011), which used the old version of RBC and that from our work, with the updated photometry in RBC. It is also found that the SED-fitting with/without fixed-metallicity from literature dose not change the agreement of the SED-fitting significantly.

Figure 8 is the same as figure 7 but for mass-to-light ratios provided by the *GALEV* models with a Kroupa (2001) IMF. The conclusion is almost the same as that in figure 7, indicating that the masses calculated from the V_0 magnitude of Table 2 of Perina et al. (2010) and Perina et al. (2011) (in the top right panel and bottom right panel, i) agrees with the values from the literatures (ii) much better than that with the masses estimated from the SED-fitting directly in our work (in the top left panel and bottom left panel, iii)

. It is mainly due to the different V_0 magnitudes of literatures and that in our work (the updated photometry are adopted), although the mass-to-light ratios may be also slightly different. Another finding is that there are some very massive clusters ($\log M/M_\odot \sim 5.5$ for the metallicity-free models and $\log M/M_\odot \sim 5.1$ for the metallicity-fixed models) predicted in the BC03 models, but we do not find those counterparts in the *GALEV* models, which is supposed to be due to the difference of the models.

5. Summary and Future Work

We have collected photometric measurements of a sample of 32 star clusters in M31, which have the SED-fitting results previously, from the *GALEX* FUV/NUV to the *WISE* mid-IR wavelength range to explore their importance for SED fits. We obtained the FUV, NUV, *UBVRI*, and 2MASS *JHK* data from the RBC v.5 catalog as well as the work of Perina et al. (2010, 2011). The *WISE* *W1/W2* band photometry was from Fan & Wang (2017), which is actually downloaded from the IPAC/IRAS website. We applied the χ^2_{\min} technique for our SED-fitting and all the upper limit of the age are set to 13.8 Gyr from Planck’s latest result. The reddening values are also from the work of Perina et al. (2010, 2011).

We based our fits on three stellar population synthesis models.

1. The currently most up-to-date Padova 2000 evolutionary tracks and the Chabrier (2003) IMF, as implemented in the BC03 models. In general, our results agree well with previous determinations, either for the metallicity-free fitting results or for the metallicity-fixed fitting results. In terms of the cluster metallicities, our values agree well with those of Chen et al. (2016). Although most cluster ages of Caldwell et al. (2011) are upper limits, their results agree reasonably well with ours.

2. We also compare the SED-fitting results derived from *GALEV* models with Kroupa (2001) IMF with the CMD-fitting results from literature. As the fitting for the BC03 models, our results agree well with previous determinations, either for the metallicity-free fitting results or for the metallicity-fixed fitting results.

3. ASPS single-star (ss-SSPs) and the binary-star simple stellar populations (bs-SSPs) model. Since the model dose not provide the *WISE* *W1/W2* band, we do not use it for the SED-fitting. It is found that a slight systematic difference between our fitting results and previous CMD-fitting determinations, either for the metallicity-free fitting results or for the metallicity-fixed fitting results, in both ss-SSPs and bs-SSPs models. This could be an important results of the paper. In particular the fact that the ages based on ss-SSPs are

also systematically different from CMD ages suggests that there may be a problem with the adopted stellar evolution models (independent from the inclusion of binaries). Actually, the “not-fitted-well” of the luminosity function, lack of reliable luminosity functions or clear main sequences, and only low limits also may lead to the age difference. For instance, overshooting and stellar binarity can affect the result obviously. The age difference between CMD fitted ages from models can be as large as a factor of 0.6 dex. Besides, the use of different isochrones (considered overshooting or not) also contributes to the age difference up to 0.4 dex as well.

Therefore, our concluding remarks are:

1. The SED-fitting from the *GALEX* FUV/NUV to the *WISE* *W1*/*W2* band of our sample 32 star clusters in M31 agree well with the previous CMD-fitting results, implying that the fitting method is reliable and reasonable.
2. The importance of the *GALEX* FUV/NUV bands are much more significant than the *WISE* *W1*/*W2* bands for the SED-fitting, which is consistent with the previous study, e.g., Fan & Wang (2017), say, the *GALEX* FUV/NUV bands effect much more significantly in the SED-fittings than the other bands, especially for the *WISE* *W1*/*W2* bands.
3. It is found that the SED-fitting results with *GALEV* models are systematically younger than the CMD-fitting results for the older clusters, i.e., ($\log t > 9.5$ yr), although for the younger clusters the agreement is well. This could be due to the model difference, which has been mentioned by many previous works, e.g., Fan & de Grijs (2012).
4. It seems that for the ASPS ss-SSPs models/bs-SSPs models, SED-fitting results are systematic older than the CMD ages (~ 0.7 dex), especially for the ages $\log t < 9.0$ (yr). It may be due to the calibration of the models, as there is no such bias for the CMD-fitting and the SED-fitting with *GALEV* and BC03 models. In fact, age difference between CMD fitted ages from different models can be as large as a factor of 0.6 and using different isochrones (e.g., considering the overshooting or not) could contribute to the age difference ~ 0.4 dex.

In the future work, we would like to carry out systematic observations to give more constraints on the age/metallicity/reddening to disentangle the parameter degeneracy. Thus, it could be helpful if there is a photometric system which is sensitive to these physical parameters, e.g., age, metallicity, reddening. The SAGE (Stellar Abundances and Galactic Evolution) survey⁶ (PI: Gang Zhao, see Fan et al. 2018; Zheng et al. 2018a,b,c) apply a brand-new SAGE photometry system, i.e., u_{SC} , v_{SAGE} , gri, DDO51 and $H\alpha_n/H\alpha_w$ for the stellar atmospheric parameters of ~ 500 million stars. The self-designed v_{SAGE} band covers

⁶<http://sage.sagenaoc.science/sagesurvey/>

the CaII H&K lines, which is very sensitive to the metallicity of the stellar populations, although it also effected by the age to some extent. The $H\alpha_n/H\alpha_w$ filters can be used to constrain the interstellar extinctions in M31, which is helpful to partly break the age-metallicity-reddening degeneracy. In the future work, we would observe with the SAGE system obtained the v_{SAGE} -band photometry of these star clusters, which could improve the precision of the metallicity estimates and helpful to determine the ages with the SED-fittings more accurately. Further, we will enlarge this small M31 GC sample to all the M31 GCs which have available photometry in all these bands (from the *GALEX* FUV/NUV to the *WISE* $W1/W2$ as well as the SAGE photometry) with the SED-fitting methods. Then the precise ages of this large sample, which is comparable to the CMD-fitting results, could be determined.

We thank the anonymous referee for his/her thorough review and helpful comments and suggestions, which significantly contributed to improving the manuscript. This research has been supported by the National Program for Key Research and Development Project (grant 2016YFA0400804) and National Key Basic Research Program of China (973 Program, grant 2015CB857002); National Natural Science Foundation of China (NFSC) through grants 11390371, 11563002, U1631102, the Sino-German Center Project GZ 1284 and the Youth Innovation Promotion Association, Chinese Academy of Sciences.

REFERENCES

- Ade, P. A. R., Aghanim, N., Arnaud, M., et al. 2016, *A&A*, 594, 13
- Anders, P., Kotulla, R., de Grijs, R., Wicker, J., 2013, *ApJ*, 778, 138
- Barmby, P., Huchra, J., Brodie, J., et al. 2000, *AJ*, 119, 727
- Bastian, N., Gieles, M., Lamers, H. J. G. L. M., et al., 2005, *A&A*, 431, 905
- Bertelli, G., Bressan, A., Chiosi, C., Fagotto, F., & Nasi, E. 1994, *A&AS*, 106, 275
- Bruzual, A., G., & Charlot, S. 2003, *MNRAS*, 344, 1000
- Bruzual, A., G. 2010, *Phil. Trans. R. Soc. A*, 368, 783
- Caldwell, N., Schiavon, R., Morrison, H., Rose, J., & Harding, P. 2011, *AJ*, 141, 61
- Cardelli, J. A., Clayton, G. C., & Mathis, J. S., 1989, *ApJ*, 345, 245

- Chabrier, G., 2003, *PASP*, 115, 763
- Chen, B. Q., Liu, X. W., Xiang, M. S., et al. 2016, *AJ*, 152, 45
- de Grijs, R., Fritze-v. Alvensleben, U., Anders, P., et al. 2003, *MNRAS*, 342, 259
- de Grijs, R., Bastian, N., Lamers, H. J. G. L. M., 2003a, *MNRAS*, 340, 197
- de Grijs, R., Anders, P., Lamers, H. J. G. L. M., et al. 2005, *MNRAS*, 359, 874
- Fan, Z., Ma, J., de Grijs, R., Yang, Y., & Zhou, X. 2006, *MNRAS*, 371, 1648
- Fan, Z., de Grijs, R., & Zhou, X. 2010, *ApJ*, 725, 200
- Fan, Z., & de Grijs, R., 2012, *MNRAS*, 424, 2009
- Fan, Z., & de Grijs, R., 2014, *ApJS*, 211, 22
- Fan, Z., de Grijs, R., Chen, B., et al. 2016, *AJ*, 152, 208
- Fan, Z., & Wang, S., 2017, *Ap&SS*, 362, 193
- Fan, Z., Zhao, G., Wang, W., et al. 2018, *Progress in Astronomy*, in press
- Galleti, S., Federici, L., Bellazzini, M., Fusi Pecci, F., & Macrina, S. 2004, *A&A*, 426, 917
- Galleti, S., Federici, L., Bellazzini, M., Buzzoni, A., & Fusi Pecci, F. 2006, *A&A*, 456, 985
- Galleti, S., Bellazzini, M., Buzzoni, L., Federici, L., & Fusi Pecci, F. 2009, *A&A*, 508, 1285
- Georgy, C., Ekström, S., Granada, A., Meynet, G., Mowlavi, N., Eggenberger, P., Maeder, A., 2013, *A&A*, 553, 24
- Girardi, L., Bertelli, G., Bressan, A., et al. 2002, *A&A*, 391, 195
- Hurley, J. R., Pols, O. R., & Tout, C. A., 2000, *MNRAS*, 315, 543.
- Hurley, J. R., Tout, C. A., & Pols, O. R., 2002, *MNRAS*, 329, 897.
- Jarrett, T. H., Cohen, M., Masci, F., et al. 2011, *ApJ*, 735, 112
- Kang, Y., Rey, S.-C., Bianchi, L., et al. 2012, *ApJS*, 199, 37
- Kotulla, R., Fritze, U., Weilbacher, P., & Anders, P., 2009, *MNRAS*, 396, 462
- Kroupa, P. 2001, *MNRAS*, 322, 231

- Kurucz, R. L. 1992, in IAU Symp. 149, The Stellar Populations of Galaxies, ed. B. Barbuy & A. Renzini (Dordrecht: Kluwer), 225
- Li, Z.-M., Han, Z.-W. 2008, MNRAS, 387, 105
- Li, Z., Mao, C., Chen, L., et al. 2012, ApJ, 761, L22
- Li, Z., Mao, C., Chen, L. 2015, ApJ, 802, 44
- Li, Z., Mao, C., Zhang, L., et al. 2016, ApJS, 225, 7
- Li, Z., Mao, C., Luo, Q., et al. 2017, RAA, 17, 71
- Li, Z., & Deng, Y. 2018, Ap&SS, 363, 97
- Luo, Q., & Li, Z. 2018, New Astronomy, 64, 61
- Lilly, T., & Fritze-v. Alvensleben, U. 2006, A&A, 457, 467
- Ma, J., Yang, Y. B., Burstein, D., et al. 2007, ApJ, 659, 359
- Ma, J., Fan, Z., de Grijs, R., et al. 2009, AJ, 137, 4884
- Ma, J., Wu, Z., Wang, S., et al. 2010, PASP, 122, 1164
- Ma, J., Wang, S., Wu, Z., et al. 2011, AJ, 141, 86
- Ma, J., Wang, S., Wu, Z., et al. 2012, AJ, 143, 29
- McConnachie, A. W., Irwin, M. J., Ferguson, A. M. N., et al. 2005, MNRAS, 356, 979
- Peacock, M. B., Maccarone, T. J., Knigge, C., et al. 2010, MNRAS, 402, 803
- Perina, S., Barmby, P., Beasley, M. A., et al. 2009a, A&A, 494, 933
- Perina, S., Federici, L., Bellazzini, M., et al. 2009b, A&A, 507, 1375
- Perina, S., Cohen, J. G., Barmby, P., et al. 2010, A&A, 511, 23
- Perina, S., Galleti, S., Fusi Pecci, F., et al. 2011, A&A, 531, 155
- Pietrinferni, A., Cassisi, S., Salaris, M., & Castelli, F. 2004, ApJ, 612, 168
- Rey, S.-C., Rich, R. M., Sohn, S. T., et al. 2007, ApJS, 173, 643
- Rich, R. M., Corsi, C. E., Cacciari, C., et al. 2005, AJ, 129, 2670

- Salpeter, E. E. 1955, ApJ, 121, 161
- Wang, S., Fan, Z., Ma, J., de Grijs, R., & Zhou, X. 2010, AJ, 139, 1438
- Wang, S., Ma, J., Fan, Z., et al. 2012, AJ, 144, 191
- Williams, B. F., & Hodge, P. W. 2001, ApJ, 548, 190
- Wright, E. L., Eisenhardt, P. R. M., Mainzer, A. K., et al. 2010, AJ, 140, 1868
- Zheng, J., Zhao, G., Wang, W., Fan, Z., Zhao, J., Tan, K. 2018, Astronomical Research & Technology, in press
- Zheng, J., Zhao, G., Wang, W., Fan, Z., Tan, K., Li C., Zuo F. 2018b, RAA, accepted
- Zheng, J., Zhao, G., Wang, W., Fan, Z., Tan, K., Li C., Zuo F. 2018c, RAA, accepted

Table 1. Ages of our sample star clusters derived from SED fits of different passband combinations with BC03 models and Padova 2000 stellar evolutionary tracks. The Chabrier (2003) IMF was adopted. For the abundance of the Sun, $Z = 0.019$ is applied for the models. The referential ages, metallicities and masses are from Perina et al. (2010, 2011).

ID	[Fe/H] (dex)	[Fe/H] _{P10/P11} (dex)	log t (Gyr)	log $t_{P10/P11}$ (Gyr)	log M (M_{\odot})	log $M_{P10/P11}$ (M_{\odot})
B015D-D041	$0.28^{+0.00}_{-1.01}$	0.00	$8.11^{+0.16}_{-0.53}$	$7.85^{+0.15}_{-0.15}$	$4.15^{+0.09}_{-0.37}$	4.20
B040-G102	$0.12^{+0.16}_{-0.78}$	0.00	$7.96^{+0.16}_{-0.19}$	$7.90^{+0.20}_{-0.15}$	$4.06^{+0.13}_{-0.15}$	4.60
B043-G106	$0.15^{+0.13}_{-1.09}$	0.00	$7.91^{+0.17}_{-0.27}$	$7.90^{+0.20}_{-0.15}$	$4.20^{+0.12}_{-0.21}$	4.40
B066-G128	$0.28^{+0.00}_{-1.38}$	0.00	$7.51^{+0.39}_{-0.52}$	$7.85^{+0.15}_{-0.15}$	$3.65^{+0.24}_{-0.39}$	4.20
B081-G142	$0.28^{+0.00}_{-0.51}$	0.00	$8.41^{+0.17}_{-0.19}$	$8.15^{+0.15}_{-0.15}$	$4.56^{+0.11}_{-0.19}$	5.10
B257D-D073	$0.28^{+0.00}_{-1.65}$	0.00	$8.11^{+0.22}_{-0.50}$	$7.90^{+0.20}_{-0.15}$	$4.18^{+0.12}_{-0.35}$	4.60
B318-G042	$0.07^{+0.21}_{-0.99}$	-0.38	$7.72^{+0.19}_{-0.15}$	$7.85^{+0.15}_{-0.15}$	$3.97^{+0.16}_{-0.09}$	3.80
B321-G046	$0.28^{+0.00}_{-0.30}$	0.68	$8.16^{+0.14}_{-0.07}$	$8.23^{+0.10}_{-0.15}$	$4.11^{+0.08}_{-0.08}$	4.20
B327-G053	$-0.20^{+0.46}_{-0.76}$	-0.38	$7.70^{+0.22}_{-0.22}$	$7.70^{+0.15}_{-0.10}$	$4.20^{+0.20}_{-0.08}$	4.50
B376-G309	$-0.06^{+0.34}_{-1.42}$	0.00	$8.06^{+0.09}_{-0.22}$	$8.00^{+0.15}_{-0.15}$	$3.90^{+0.10}_{-0.13}$	4.10
B448-D035	$-1.63^{+0.85}_{0.00}$	0.00	$8.71^{+0.26}_{-0.19}$	$7.90^{+0.20}_{-0.15}$	$4.48^{+0.20}_{-0.11}$	4.10
B475-V128	$-0.90^{+0.83}_{-0.73}$	-0.38	$8.56^{+0.24}_{-0.29}$	$8.30^{+0.20}_{-0.20}$	$4.51^{+0.28}_{-0.14}$	4.70
V031	$-0.12^{+0.40}_{-1.17}$	-0.68	$8.81^{+0.28}_{-0.70}$	$8.45^{+0.15}_{-0.15}$	$4.39^{+0.28}_{-0.52}$	4.80
VDB0-B195D	$-0.07^{+0.19}_{-0.71}$	0.00	$7.91^{+0.08}_{-0.21}$	$7.40^{+0.30}_{-0.30}$	$4.98^{+0.08}_{-0.15}$	99.99
B083-G146	$-1.63^{+0.13}_{0.00}$	-0.38	$10.14^{+0.00}_{-0.09}$	$8.70^{+1.44}_{0.00}$	$5.47^{+0.00}_{-0.09}$	4.70
B222-G277	$-0.83^{+0.19}_{-0.18}$	0.00	$9.16^{+0.14}_{-0.01}$	$8.60^{+1.54}_{0.00}$	$4.51^{+0.25}_{-0.01}$	4.60
B347-G154	$-1.63^{+0.13}_{0.00}$	-0.38	$10.03^{+0.04}_{-0.02}$	$8.80^{+1.34}_{0.00}$	$5.44^{+0.03}_{-0.02}$	4.70
B374-G306	$-1.63^{+0.37}_{0.00}$	0.00	$8.81^{+0.10}_{-0.28}$	$8.50^{+1.64}_{0.00}$	$4.17^{+0.06}_{-0.20}$	3.90
NB16	$0.28^{+0.00}_{-0.16}$	0.00	$9.21^{+0.62}_{-0.03}$	$8.70^{+1.44}_{0.00}$	$4.88^{+0.57}_{-0.09}$	4.80
B049-G112	$0.27^{+0.01}_{-0.40}$	0.00	$8.56^{+0.10}_{-0.15}$	$8.45^{+0.20}_{-0.20}$	$4.45^{+0.07}_{-0.15}$	4.50
B367-G292	$0.22^{+0.06}_{-0.17}$	0.00	$8.31^{+0.06}_{-0.06}$	$8.30^{+0.20}_{-0.20}$	$4.02^{+0.04}_{-0.06}$	4.30
B458-D049	$0.28^{+0.00}_{-0.87}$	0.00	$8.56^{+0.16}_{-0.36}$	$8.50^{+0.20}_{-0.20}$	$4.28^{+0.12}_{-0.34}$	4.10
B521-SK034A	$-0.21^{+0.16}_{-0.75}$	0.00	$7.96^{+0.10}_{-0.16}$	$8.60^{+0.30}_{-0.30}$	$3.72^{+0.10}_{-0.11}$	3.90
M039	$-1.23^{+1.51}_{-0.40}$	0.00	$8.41^{+0.66}_{-0.68}$	$8.50^{+0.20}_{-0.20}$	$3.40^{+0.64}_{-0.24}$	3.80
M050	$0.28^{+0.00}_{-1.91}$	0.00	$8.16^{+0.32}_{-0.78}$	$8.75^{+0.30}_{-0.30}$	$3.57^{+0.18}_{-0.44}$	4.30
B315-G038	$-1.39^{+1.06}_{-0.24}$	-0.38	$8.01^{+0.04}_{-0.19}$	$8.00^{+0.15}_{-0.20}$	$4.62^{+0.04}_{-0.08}$	4.60
B319-G044	$-1.57^{+0.88}_{-0.06}$	-0.38	$8.01^{+0.15}_{-0.20}$	$8.00^{+0.15}_{-0.20}$	$4.03^{+0.06}_{-0.12}$	3.90
B342-G094	$-0.09^{+0.37}_{-1.07}$	-0.38	$8.06^{+0.21}_{-0.22}$	$8.20^{+0.15}_{-0.20}$	$3.90^{+0.17}_{-0.17}$	4.00
B368-G293	$0.28^{+0.00}_{-1.11}$	0.00	$7.36^{+0.61}_{-0.50}$	$7.80^{+0.10}_{-0.10}$	$3.49^{+0.35}_{-0.55}$	4.40
B292-G010	$-0.91^{+0.15}_{-0.23}$	-1.80	$9.11^{+0.01}_{-0.04}$	$9.80^{+0.34}_{0.00}$	$4.56^{+0.05}_{-0.02}$	99.99

Table 1—Continued

ID	[Fe/H] (dex)	[Fe/H] _{P10/P11} (dex)	log t (Gyr)	log $t_{\text{P10/P11}}$ (Gyr)	log M (M_{\odot})	log M _{P10/P11} (M_{\odot})
B337-G068	$-1.45^{+0.13}_{-0.14}$	-1.28	$10.14^{+0.00}_{-0.06}$	$9.65^{+0.49}_{0.00}$	$5.41^{+0.00}_{-0.05}$	99.99
B350-G162	$-1.63^{+0.08}_{0.00}$	-1.50	$10.14^{+0.00}_{-0.04}$	$9.75^{+0.39}_{0.00}$	$5.49^{+0.00}_{-0.04}$	99.99

Table 2. Same as Table 1 but for fixed-Z from literatures.

ID	[Fe/H] _{P10/P11} (dex)	log <i>t</i> (Gyr)	log <i>t</i> _{P10/P11} (Gyr)	log M (<i>M</i> _⊙)	log M _{P10/P11} (<i>M</i> _⊙)
B015D-D041	0.00	8.11 ^{+0.25} _{-0.34}	7.85 ^{+0.15} _{-0.15}	4.10 ^{+0.15} _{-0.21}	4.20
B040-G102	0.00	7.96 ^{+0.19} _{-0.17}	7.90 ^{+0.20} _{-0.15}	4.04 ^{+0.13} _{-0.10}	4.60
B043-G106	0.00	7.96 ^{+0.14} _{-0.22}	7.90 ^{+0.20} _{-0.15}	4.19 ^{+0.10} _{-0.13}	4.40
B066-G128	0.00	7.54 ^{+0.40} _{-0.56}	7.85 ^{+0.15} _{-0.15}	3.70 ^{+0.15} _{-0.42}	4.20
B081-G142	0.00	8.51 ^{+0.19} _{-0.23}	8.15 ^{+0.15} _{-0.15}	4.59 ^{+0.12} _{-0.14}	5.10
B257D-D073	0.00	8.16 ^{+0.28} _{-0.52}	7.90 ^{+0.20} _{-0.15}	4.17 ^{+0.17} _{-0.29}	4.60
B318-G042	-0.38	7.81 ^{+0.19} _{-0.23}	7.85 ^{+0.15} _{-0.15}	3.99 ^{+0.08} _{-0.12}	3.80
B321-G046	0.68	8.16 ^{+0.14} _{-0.07}	8.23 ^{+0.10} _{-0.15}	4.11 ^{+0.08} _{-0.04}	4.20
B327-G053	-0.38	7.70 ^{+0.24} _{-0.23}	7.70 ^{+0.15} _{-0.10}	4.19 ^{+0.12} _{-0.14}	4.50
B376-G309	0.00	8.06 ^{+0.09} _{-0.25}	8.00 ^{+0.15} _{-0.15}	3.91 ^{+0.06} _{-0.17}	4.10
B448-D035	0.00	8.36 ^{+0.20} _{-0.10}	7.90 ^{+0.20} _{-0.15}	4.38 ^{+0.12} _{-0.06}	4.10
B475-V128	-0.38	8.46 ^{+0.18} _{-0.28}	8.30 ^{+0.20} _{-0.20}	4.50 ^{+0.12} _{-0.17}	4.70
V031	-0.68	9.06 ^{+0.38} _{-0.77}	8.45 ^{+0.15} _{-0.15}	4.49 ^{+0.27} _{-0.51}	4.80
VDB0-B195D	0.00	7.86 ^{+0.11} _{-0.16}	7.40 ^{+0.30} _{-0.30}	4.96 ^{+0.06} _{-0.09}	99.99
B083-G146	-0.38	8.96 ^{+0.11} _{-0.11}	8.70 ^{+1.44} _{0.00}	4.70 ^{+0.05} _{-0.09}	4.70
B222-G277	0.00	8.96 ^{+0.11} _{-0.14}	8.60 ^{+1.54} _{0.00}	4.63 ^{+0.08} _{-0.11}	4.60
B347-G154	-0.38	9.06 ^{+0.03} _{-0.06}	8.80 ^{+1.34} _{0.00}	4.81 ^{+0.00} _{-0.02}	4.70
B374-G306	0.00	8.41 ^{+0.19} _{-0.18}	8.50 ^{+1.64} _{0.00}	4.03 ^{+0.12} _{-0.11}	3.90
NB16	0.00	9.54 ^{+0.59} _{-0.39}	8.70 ^{+1.44} _{0.00}	5.13 ^{+0.47} _{-0.40}	4.80
B049-G112	0.00	8.66 ^{+0.10} _{-0.14}	8.45 ^{+0.20} _{-0.20}	4.49 ^{+0.07} _{-0.09}	4.50
B367-G292	0.00	8.36 ^{+0.09} _{-0.06}	8.30 ^{+0.20} _{-0.20}	4.03 ^{+0.06} _{-0.03}	4.30
B458-D049	0.00	8.61 ^{+0.22} _{-0.33}	8.50 ^{+0.20} _{-0.20}	4.28 ^{+0.15} _{-0.20}	4.10
B521-SK034A	0.00	7.81 ^{+0.15} _{-0.12}	8.60 ^{+0.30} _{-0.30}	3.66 ^{+0.09} _{-0.06}	3.90
M039	0.00	8.26 ^{+0.46} _{-0.57}	8.50 ^{+0.20} _{-0.20}	3.44 ^{+0.28} _{-0.35}	3.80
M050	0.00	8.26 ^{+0.34} _{-0.89}	8.75 ^{+0.30} _{-0.30}	3.59 ^{+0.21} _{-0.46}	4.30
B315-G038	-0.38	7.91 ^{+0.15} _{-0.24}	8.00 ^{+0.15} _{-0.20}	4.58 ^{+0.07} _{-0.13}	4.60
B319-G044	-0.38	7.76 ^{+0.28} _{-0.28}	8.00 ^{+0.15} _{-0.20}	3.90 ^{+0.13} _{-0.17}	3.90
B342-G094	-0.38	8.06 ^{+0.27} _{-0.23}	8.20 ^{+0.15} _{-0.20}	3.86 ^{+0.15} _{-0.11}	4.00
B368-G293	0.00	7.59 ^{+0.46} _{-0.75}	7.80 ^{+0.10} _{-0.10}	3.61 ^{+0.23} _{-0.69}	4.40
B292-G010	-1.80	9.36 ^{+0.14} _{-0.14}	9.80 ^{+0.34} _{0.00}	4.74 ^{+0.10} _{-0.08}	99.99

Table 2—Continued

ID	[Fe/H] _{P10/P11} (dex)	log t (Gyr)	log $t_{\text{P10/P11}}$ (Gyr)	log M (M_{\odot})	log M _{P10/P11} (M_{\odot})
B337-G068	-1.28	$10.14^{+0.00}_{-0.08}$	$9.65^{+0.49}_{0.00}$	$5.42^{+0.00}_{-0.06}$	99.99
B350-G162	-1.50	$10.14^{+0.00}_{-0.06}$	$9.75^{+0.39}_{0.00}$	$5.48^{+0.00}_{-0.05}$	99.99

Table 3. Same as Table 1 but for the *GALEV* Models and a Kroupa (2001) IMF.
 $Z = 0.02$ (solar metallicity) is adopted for the models.

ID	[Fe/H] (dex)	[Fe/H] _{P10/P11} (dex)	log t (Gyr)	log $t_{P10/P11}$ (Gyr)	log M (M_{\odot})	log M _{P10/P11} (M_{\odot})
B015D-D041	$-0.35^{+0.12}_{-1.06}$	-0.02	$8.03^{+0.03}_{-0.07}$	$7.85^{+0.15}_{-0.15}$	$4.05^{+0.04}_{-0.05}$	4.20
B040-G102	$-0.35^{+0.21}_{-0.72}$	-0.02	$8.00^{+0.07}_{-0.16}$	$7.90^{+0.20}_{-0.15}$	$4.07^{+0.08}_{-0.08}$	4.60
B043-G106	$-0.38^{+0.16}_{-0.92}$	-0.02	$7.96^{+0.06}_{-0.20}$	$7.90^{+0.20}_{-0.15}$	$4.20^{+0.05}_{-0.11}$	4.40
B066-G128	$0.40^{+0.00}_{-1.25}$	-0.02	$7.45^{+0.30}_{-0.34}$	$7.85^{+0.15}_{-0.15}$	$3.73^{+0.14}_{-0.38}$	4.20
B081-G142	$-1.38^{+0.66}_{-0.32}$	-0.02	$8.70^{+0.21}_{-0.35}$	$8.15^{+0.15}_{-0.15}$	$4.59^{+0.18}_{-0.28}$	5.10
B257D-D073	$-0.10^{+0.50}_{-1.07}$	-0.02	$8.06^{+0.32}_{-0.22}$	$7.90^{+0.20}_{-0.15}$	$4.15^{+0.25}_{-0.16}$	4.60
B318-G042	$-0.42^{+0.32}_{-0.85}$	-0.40	$7.86^{+0.13}_{-0.28}$	$7.85^{+0.15}_{-0.15}$	$4.06^{+0.10}_{-0.15}$	3.80
B321-G046	$-0.31^{+0.22}_{-0.56}$	0.65	$8.06^{+0.07}_{-0.04}$	$8.23^{+0.10}_{-0.15}$	$4.01^{+0.08}_{-0.06}$	4.20
B327-G053	$-0.38^{+0.38}_{-0.69}$	-0.40	$7.68^{+0.26}_{-0.24}$	$7.70^{+0.15}_{-0.10}$	$4.21^{+0.21}_{-0.12}$	4.50
B376-G309	$-0.38^{+0.78}_{-0.97}$	-0.02	$8.00^{+0.17}_{-0.20}$	$8.00^{+0.15}_{-0.15}$	$3.86^{+0.22}_{-0.09}$	4.10
B448-D035	$0.40^{+0.00}_{-0.75}$	-0.02	$8.29^{+0.08}_{-0.20}$	$7.90^{+0.20}_{-0.15}$	$4.44^{+0.04}_{-0.22}$	4.10
B475-V128	$-1.70^{+0.54}_{0.00}$	-0.40	$8.70^{+0.30}_{-0.68}$	$8.30^{+0.20}_{-0.20}$	$4.57^{+0.20}_{-0.31}$	4.70
V031	$0.40^{+0.00}_{-1.33}$	-0.70	$8.20^{+0.38}_{-0.33}$	$8.45^{+0.15}_{-0.15}$	$4.13^{+0.24}_{-0.30}$	4.80
VDB0-B195D	$-0.38^{+0.04}_{-0.51}$	-0.02	$7.92^{+0.07}_{-0.19}$	$7.40^{+0.30}_{-0.30}$	$5.01^{+0.03}_{-0.14}$	99.99
B083-G146	$-1.70^{+0.26}_{0.00}$	-0.40	$9.30^{+0.16}_{-0.07}$	$8.70^{+1.44}_{0.00}$	$4.76^{+0.14}_{-0.03}$	4.70
B222-G277	$-0.31^{+0.15}_{-0.14}$	-0.02	$8.96^{+0.04}_{-0.04}$	$8.60^{+1.54}_{0.00}$	$4.59^{+0.05}_{-0.04}$	4.60
B347-G154	$-1.63^{+0.27}_{-0.07}$	-0.40	$9.46^{+0.08}_{-0.07}$	$8.80^{+1.34}_{0.00}$	$4.96^{+0.07}_{-0.06}$	4.70
B374-G306	$-0.06^{+0.46}_{-0.54}$	-0.02	$8.40^{+0.18}_{-0.26}$	$8.50^{+1.64}_{0.00}$	$4.05^{+0.19}_{-0.23}$	3.90
NB16	$0.08^{+0.19}_{-0.50}$	-0.02	$9.24^{+0.32}_{-0.24}$	$8.70^{+1.44}_{0.00}$	$4.94^{+0.32}_{-0.34}$	4.80
B049-G112	$-0.42^{+0.35}_{-1.27}$	-0.02	$8.70^{+0.16}_{-0.27}$	$8.45^{+0.20}_{-0.20}$	$4.48^{+0.17}_{-0.34}$	4.50
B367-G292	$0.40^{+0.00}_{-0.11}$	-0.02	$8.19^{+0.06}_{-0.03}$	$8.30^{+0.20}_{-0.20}$	$4.03^{+0.03}_{-0.04}$	4.30
B458-D049	$0.01^{+0.24}_{-0.15}$	-0.02	$8.50^{+0.15}_{-0.12}$	$8.50^{+0.20}_{-0.20}$	$4.23^{+0.15}_{-0.08}$	4.10
B521-SK034A	$-0.38^{+0.05}_{-0.57}$	-0.02	$7.96^{+0.04}_{-0.05}$	$8.60^{+0.30}_{-0.30}$	$3.76^{+0.02}_{-0.02}$	3.90
M039	$-0.21^{+0.60}_{-1.49}$	-0.02	$8.34^{+0.40}_{-0.69}$	$8.50^{+0.20}_{-0.20}$	$3.50^{+0.36}_{-0.37}$	3.80
M050	$0.40^{+0.00}_{-0.33}$	-0.02	$7.90^{+0.36}_{-0.13}$	$8.75^{+0.30}_{-0.30}$	$3.49^{+0.20}_{-0.13}$	4.30
B315-G038	$-1.41^{+0.57}_{-0.28}$	-0.40	$8.00^{+0.02}_{-0.18}$	$8.00^{+0.15}_{-0.20}$	$4.67^{+0.00}_{-0.11}$	4.60
B319-G044	$-1.56^{+0.83}_{-0.14}$	-0.40	$8.00^{+0.04}_{-0.29}$	$8.00^{+0.15}_{-0.20}$	$4.07^{+0.02}_{-0.20}$	3.90
B342-G094	$-0.38^{+0.72}_{-0.96}$	-0.40	$8.00^{+0.08}_{-0.16}$	$8.20^{+0.15}_{-0.20}$	$3.87^{+0.16}_{-0.07}$	4.00
B368-G293	$0.40^{+0.00}_{-0.48}$	-0.02	$7.30^{+0.45}_{-0.27}$	$7.80^{+0.10}_{-0.10}$	$3.57^{+0.22}_{-0.43}$	4.40
B292-G010	$-1.70^{+0.23}_{0.00}$	-1.82	$9.24^{+0.06}_{-0.12}$	$9.80^{+0.34}_{0.00}$	$4.62^{+0.04}_{-0.12}$	99.99

Table 3—Continued

ID	[Fe/H] (dex)	[Fe/H] _{P10/P11} (dex)	log t (Gyr)	log $t_{\text{P10/P11}}$ (Gyr)	log M (M_{\odot})	log M _{P10/P11} (M_{\odot})
B337-G068	$-1.09^{+0.13}_{-0.20}$	-1.30	$9.27^{+0.07}_{-0.07}$	$9.65^{+0.49}_{0.00}$	$4.78^{+0.06}_{-0.05}$	99.99
B350-G162	$-1.63^{+0.20}_{-0.07}$	-1.52	$9.31^{+0.08}_{-0.04}$	$9.75^{+0.39}_{0.00}$	$4.79^{+0.08}_{-0.02}$	99.99

Table 4. Same as Table 3 but for fixed-Z from literatures.

ID	[Fe/H] _{P10/P11} (dex)	log t (Gyr)	log $t_{P10/P11}$ (Gyr)	log M (M_{\odot})	log M _{P10/P11} (M_{\odot})
B015D-D041	-0.02	$7.83^{+0.05}_{-0.28}$	$7.85^{+0.15}_{-0.15}$	$3.99^{+0.03}_{-0.15}$	4.20
B040-G102	-0.02	$7.81^{+0.27}_{-0.21}$	$7.90^{+0.20}_{-0.15}$	$4.01^{+0.16}_{-0.12}$	4.60
B043-G106	-0.02	$7.81^{+0.09}_{-0.22}$	$7.90^{+0.20}_{-0.15}$	$4.16^{+0.06}_{-0.13}$	4.40
B066-G128	-0.02	$7.51^{+0.45}_{-0.63}$	$7.85^{+0.15}_{-0.15}$	$3.68^{+0.24}_{-0.72}$	4.20
B081-G142	-0.02	$8.43^{+0.23}_{-0.53}$	$8.15^{+0.15}_{-0.15}$	$4.57^{+0.14}_{-0.29}$	5.10
B257D-D073	-0.02	$7.98^{+0.40}_{-0.16}$	$7.90^{+0.20}_{-0.15}$	$4.11^{+0.23}_{-0.09}$	4.60
B318-G042	-0.40	$7.78^{+0.20}_{-0.28}$	$7.85^{+0.15}_{-0.15}$	$4.01^{+0.10}_{-0.18}$	3.80
B321-G046	0.65	$7.75^{+0.03}_{-0.15}$	$8.23^{+0.10}_{-0.15}$	$3.94^{+0.02}_{-0.07}$	4.20
B327-G053	-0.40	$7.68^{+0.26}_{-0.24}$	$7.70^{+0.15}_{-0.10}$	$4.21^{+0.15}_{-0.14}$	4.50
B376-G309	-0.02	$7.94^{+0.36}_{-0.29}$	$8.00^{+0.15}_{-0.15}$	$3.89^{+0.21}_{-0.18}$	4.10
B448-D035	-0.02	$8.47^{+0.08}_{-0.27}$	$7.90^{+0.20}_{-0.15}$	$4.47^{+0.05}_{-0.16}$	4.10
B475-V128	-0.40	$8.02^{+0.06}_{-0.35}$	$8.30^{+0.20}_{-0.20}$	$4.28^{+0.04}_{-0.19}$	4.70
V031	-0.70	$8.50^{+0.46}_{-0.41}$	$8.45^{+0.15}_{-0.15}$	$4.14^{+0.29}_{-0.22}$	4.80
VDB0-B195D	-0.02	$7.78^{+0.04}_{-0.20}$	$7.40^{+0.30}_{-0.30}$	$4.96^{+0.03}_{-0.11}$	99.99
B083-G146	-0.40	$8.88^{+0.11}_{-0.18}$	$8.70^{+1.44}_{0.00}$	$4.67^{+0.06}_{-0.11}$	4.70
B222-G277	-0.02	$8.86^{+0.05}_{-0.06}$	$8.60^{+1.54}_{0.00}$	$4.59^{+0.04}_{-0.05}$	4.60
B347-G154	-0.40	$8.92^{+0.07}_{-0.07}$	$8.80^{+1.34}_{0.00}$	$4.76^{+0.04}_{-0.04}$	4.70
B374-G306	-0.02	$8.40^{+0.17}_{-0.26}$	$8.50^{+1.64}_{0.00}$	$4.05^{+0.10}_{-0.15}$	3.90
NB16	-0.02	$9.08^{+0.66}_{-0.06}$	$8.70^{+1.44}_{0.00}$	$4.75^{+0.59}_{-0.05}$	4.80
B049-G112	-0.02	$8.49^{+0.21}_{-0.11}$	$8.45^{+0.20}_{-0.20}$	$4.40^{+0.15}_{-0.05}$	4.50
B367-G292	-0.02	$8.37^{+0.06}_{-0.05}$	$8.30^{+0.20}_{-0.20}$	$4.06^{+0.03}_{-0.02}$	4.30
B458-D049	-0.02	$8.52^{+0.16}_{-0.14}$	$8.50^{+0.20}_{-0.20}$	$4.24^{+0.11}_{-0.07}$	4.10
B521-SK034A	-0.02	$7.81^{+0.05}_{-0.11}$	$8.60^{+0.30}_{-0.30}$	$3.72^{+0.03}_{-0.08}$	3.90
M039	-0.02	$8.26^{+0.43}_{-0.31}$	$8.50^{+0.20}_{-0.20}$	$3.47^{+0.26}_{-0.17}$	3.80
M050	-0.02	$8.15^{+0.31}_{-0.26}$	$8.75^{+0.30}_{-0.30}$	$3.56^{+0.17}_{-0.14}$	4.30
B315-G038	-0.40	$7.86^{+0.14}_{-0.34}$	$8.00^{+0.15}_{-0.20}$	$4.60^{+0.06}_{-0.22}$	4.60
B319-G044	-0.40	$7.78^{+0.22}_{-0.38}$	$8.00^{+0.15}_{-0.20}$	$3.94^{+0.11}_{-0.23}$	3.90
B342-G094	-0.40	$8.00^{+0.08}_{-0.16}$	$8.20^{+0.15}_{-0.20}$	$3.87^{+0.05}_{-0.07}$	4.00
B368-G293	-0.02	$7.56^{+0.49}_{-0.67}$	$7.80^{+0.10}_{-0.10}$	$3.61^{+0.27}_{-0.73}$	4.40
B292-G010	-1.82	$9.24^{+0.06}_{-0.12}$	$9.80^{+0.34}_{0.00}$	$4.62^{+0.02}_{-0.12}$	99.99

Table 4—Continued

ID	[Fe/H] _{P10/P11} (dex)	log t (Gyr)	log $t_{\text{P10/P11}}$ (Gyr)	log M (M_{\odot})	log M _{P10/P11} (M_{\odot})
B337-G068	-1.30	$9.30^{+0.13}_{-0.04}$	$9.65^{+0.49}_{0.00}$	$4.75^{+0.09}_{-0.01}$	99.99
B350-G162	-1.52	$9.30^{+0.08}_{-0.04}$	$9.75^{+0.39}_{0.00}$	$4.79^{+0.06}_{-0.01}$	99.99

Table 5. Same as Table 1 but for the ASPS bsp-SSPs Models. $Z = 0.02$ (solar metallicity) is adopted for the models.

ID	[Fe/H] (dex)	[Fe/H] _{P10/P11} (dex)	log t (Gyr)	log t_{P10} (Gyr)
B015D-D041	$-1.32^{+0.94}_{-0.50}$	-0.02	$9.63^{+0.46}_{-1.41}$	$7.85^{+0.15}_{-0.15}$
B040-G102	$-0.32^{+0.38}_{-0.62}$	-0.02	$8.90^{+0.30}_{-0.22}$	$7.90^{+0.20}_{-0.15}$
B043-G106	$-0.02^{+0.20}_{-0.46}$	-0.02	$8.70^{+0.17}_{-0.18}$	$7.90^{+0.20}_{-0.15}$
B066-G128	$0.18^{+0.00}_{-0.78}$	-0.02	$8.60^{+0.15}_{-0.29}$	$7.85^{+0.15}_{-0.15}$
B081-G142	$-1.42^{+0.88}_{-0.40}$	-0.02	$9.68^{+0.42}_{-0.25}$	$8.15^{+0.15}_{-0.15}$
B257D-D073	$0.18^{+0.00}_{-0.67}$	-0.02	$8.78^{+0.27}_{-0.29}$	$7.90^{+0.20}_{-0.15}$
B318-G042	$0.08^{+0.10}_{-0.59}$	-0.40	$8.60^{+0.14}_{-0.19}$	$7.85^{+0.15}_{-0.15}$
B321-G046	$0.18^{+0.00}_{-0.35}$	0.65	$8.78^{+0.18}_{-0.16}$	$8.23^{+0.10}_{-0.15}$
B327-G053	$0.08^{+0.10}_{-0.55}$	-0.40	$8.60^{+0.16}_{-0.18}$	$7.70^{+0.15}_{-0.10}$
B376-G309	$-0.02^{+0.20}_{-0.69}$	-0.02	$8.85^{+0.46}_{-0.27}$	$8.00^{+0.15}_{-0.15}$
B448-D035	$0.18^{+0.00}_{-0.33}$	-0.02	$8.95^{+0.25}_{-0.11}$	$7.90^{+0.20}_{-0.15}$
B475-V128	$-1.12^{+0.81}_{-0.70}$	-0.40	$9.63^{+0.49}_{-0.22}$	$8.30^{+0.20}_{-0.20}$
V031	$-0.02^{+0.20}_{-1.80}$	-0.70	$9.97^{+0.17}_{-1.11}$	$8.45^{+0.15}_{-0.15}$
VDB0-B195D	$-0.02^{+0.20}_{-0.49}$	-0.02	$8.70^{+0.12}_{-0.18}$	$7.40^{+0.30}_{-0.30}$
B083-G146	$-0.12^{+0.20}_{-1.03}$	-0.40	$9.97^{+0.14}_{-0.01}$	$8.70^{+1.44}_{0.00}$
B222-G277	$-0.02^{+0.17}_{-1.11}$	-0.02	$10.11^{+0.03}_{-0.79}$	$8.60^{+1.54}_{0.00}$
B347-G154	$-0.12^{+0.21}_{-0.59}$	-0.40	$9.97^{+0.15}_{-0.01}$	$8.80^{+1.34}_{0.00}$
B374-G306	$0.18^{+0.00}_{-0.58}$	-0.02	$9.04^{+0.72}_{-0.24}$	$8.50^{+1.64}_{0.00}$
NB16	$0.18^{+0.00}_{-0.76}$	-0.02	$9.62^{+0.31}_{-0.02}$	$8.70^{+1.44}_{0.00}$
B049-G112	$-1.22^{+0.93}_{-0.60}$	-0.02	$9.91^{+0.23}_{-0.53}$	$8.45^{+0.20}_{-0.20}$
B367-G292	$-0.92^{+0.45}_{-0.31}$	-0.02	$9.41^{+0.71}_{-0.29}$	$8.30^{+0.20}_{-0.20}$
B458-D049	$0.18^{+0.00}_{-0.79}$	-0.02	$9.15^{+0.72}_{-0.65}$	$8.50^{+0.20}_{-0.20}$
B521-SK034A	$-0.32^{+0.50}_{-1.50}$	-0.02	$8.78^{+0.64}_{-0.83}$	$8.60^{+0.30}_{-0.30}$
M039	$0.18^{+0.00}_{-2.00}$	-0.02	$8.95^{+0.80}_{-0.73}$	$8.50^{+0.20}_{-0.20}$
M050	$-0.92^{+1.10}_{-0.90}$	-0.02	$9.15^{+0.98}_{-0.25}$	$8.75^{+0.30}_{-0.30}$
B315-G038	$-0.02^{+0.20}_{-0.63}$	-0.40	$8.70^{+0.12}_{-0.24}$	$8.00^{+0.15}_{-0.20}$
B319-G044	$-0.52^{+0.44}_{-0.34}$	-0.40	$8.90^{+0.16}_{-0.10}$	$8.00^{+0.15}_{-0.20}$
B342-G094	$-0.22^{+0.30}_{-0.64}$	-0.40	$8.90^{+0.09}_{-0.24}$	$8.20^{+0.15}_{-0.20}$
B368-G293	$0.18^{+0.00}_{-1.18}$	-0.02	$8.60^{+0.19}_{-0.32}$	$7.80^{+0.10}_{-0.10}$
B292-G010	$-0.02^{+0.20}_{-0.21}$	-1.82	$9.97^{+0.13}_{-0.01}$	$9.80^{+0.34}_{0.00}$

Table 5—Continued

ID	[Fe/H] (dex)	[Fe/H] _{P10/P11} (dex)	log t (Gyr)	log t_{P10} (Gyr)
B337-G068	$-0.12^{+0.21}_{-0.15}$	-1.30	$10.11^{+0.01}_{-0.00}$	$9.65^{+0.49}_{0.00}$
B350-G162	$-0.12^{+0.28}_{-0.15}$	-1.52	$9.97^{+0.14}_{-0.01}$	$9.75^{+0.39}_{0.00}$

Table 6. Same as Table 5 but for fixed-Z from literatures.

ID	[Fe/H] _{P10/P11} (dex)	log t (Gyr)	log $t_{P10/P11}$ (Gyr)
B015D-D041	-0.02	$8.95^{+1.18}_{-0.95}$	$7.85^{+0.15}_{-0.15}$
B040-G102	-0.02	$8.78^{+0.16}_{-0.22}$	$7.90^{+0.20}_{-0.15}$
B043-G106	-0.02	$8.70^{+0.17}_{-0.18}$	$7.90^{+0.20}_{-0.15}$
B066-G128	-0.02	$8.70^{+0.12}_{-0.31}$	$7.85^{+0.15}_{-0.15}$
B081-G142	-0.02	$9.11^{+0.41}_{-0.32}$	$8.15^{+0.15}_{-0.15}$
B257D-D073	-0.02	$8.85^{+0.46}_{-0.29}$	$7.90^{+0.20}_{-0.15}$
B318-G042	-0.40	$8.85^{+0.12}_{-0.27}$	$7.85^{+0.15}_{-0.15}$
B321-G046	0.65	$8.78^{+0.18}_{-0.16}$	$8.23^{+0.10}_{-0.15}$
B327-G053	-0.40	$8.85^{+0.12}_{-0.27}$	$7.70^{+0.15}_{-0.10}$
B376-G309	-0.02	$8.85^{+0.46}_{-0.27}$	$8.00^{+0.15}_{-0.15}$
B448-D035	-0.02	$9.00^{+0.22}_{-0.09}$	$7.90^{+0.20}_{-0.15}$
B475-V128	-0.40	$9.28^{+0.46}_{-0.13}$	$8.30^{+0.20}_{-0.20}$
V031	-0.70	$9.15^{+0.99}_{-0.11}$	$8.45^{+0.15}_{-0.15}$
VDB0-B195D	-0.02	$8.70^{+0.12}_{-0.18}$	$7.40^{+0.30}_{-0.30}$
B083-G146	-0.40	$9.96^{+0.18}_{-0.16}$	$8.70^{+1.44}_{0.00}$
B222-G277	-0.02	$10.11^{+0.03}_{-0.79}$	$8.60^{+1.54}_{0.00}$
B347-G154	-0.40	$10.13^{+0.01}_{-0.33}$	$8.80^{+1.34}_{0.00}$
B374-G306	-0.02	$9.11^{+0.86}_{-0.26}$	$8.50^{+1.64}_{0.00}$
NB16	-0.02	$9.68^{+0.46}_{-0.36}$	$8.70^{+1.44}_{0.00}$
B049-G112	-0.02	$9.26^{+0.72}_{-0.07}$	$8.45^{+0.20}_{-0.20}$
B367-G292	-0.02	$8.95^{+0.36}_{-0.15}$	$8.30^{+0.20}_{-0.20}$
B458-D049	-0.02	$9.15^{+0.97}_{-0.66}$	$8.50^{+0.20}_{-0.20}$
B521-SK034A	-0.02	$8.70^{+1.44}_{-0.79}$	$8.60^{+0.30}_{-0.30}$
M039	-0.02	$8.90^{+1.07}_{-0.68}$	$8.50^{+0.20}_{-0.20}$
M050	-0.02	$8.78^{+1.33}_{-0.37}$	$8.75^{+0.30}_{-0.30}$
B315-G038	-0.40	$8.90^{+0.09}_{-0.33}$	$8.00^{+0.15}_{-0.20}$
B319-G044	-0.40	$8.85^{+0.18}_{-0.07}$	$8.00^{+0.15}_{-0.20}$
B342-G094	-0.40	$8.95^{+0.25}_{-0.21}$	$8.20^{+0.15}_{-0.20}$
B368-G293	-0.02	$8.70^{+0.19}_{-0.41}$	$7.80^{+0.10}_{-0.10}$
B292-G010	-1.82	$9.96^{+0.16}_{-0.38}$	$9.80^{+0.34}_{0.00}$

Table 6—Continued

ID	[Fe/H] _{P10/P11} (dex)	log t (Gyr)	log $t_{\text{P10/P11}}$ (Gyr)
B337-G068	-1.30	$10.00^{+0.12}_{-0.17}$	$9.65^{+0.49}_{0.00}$
B350-G162	-1.52	$10.00^{+0.13}_{-0.35}$	$9.75^{+0.39}_{0.00}$

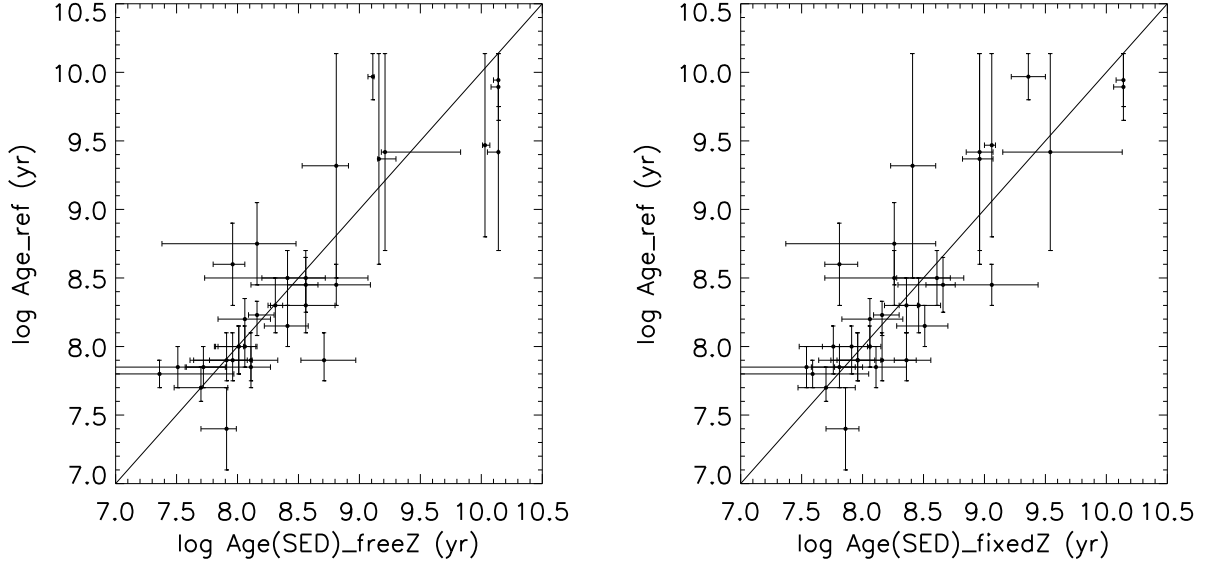


Fig. 1.— Age comparisons resulting from fits employing the BC03 models using all-band photometry with free-Z (left) and those with fixed-Z (right). Padova 2000 evolutionary tracks and a Chabrier (2003) IMF are adopted.

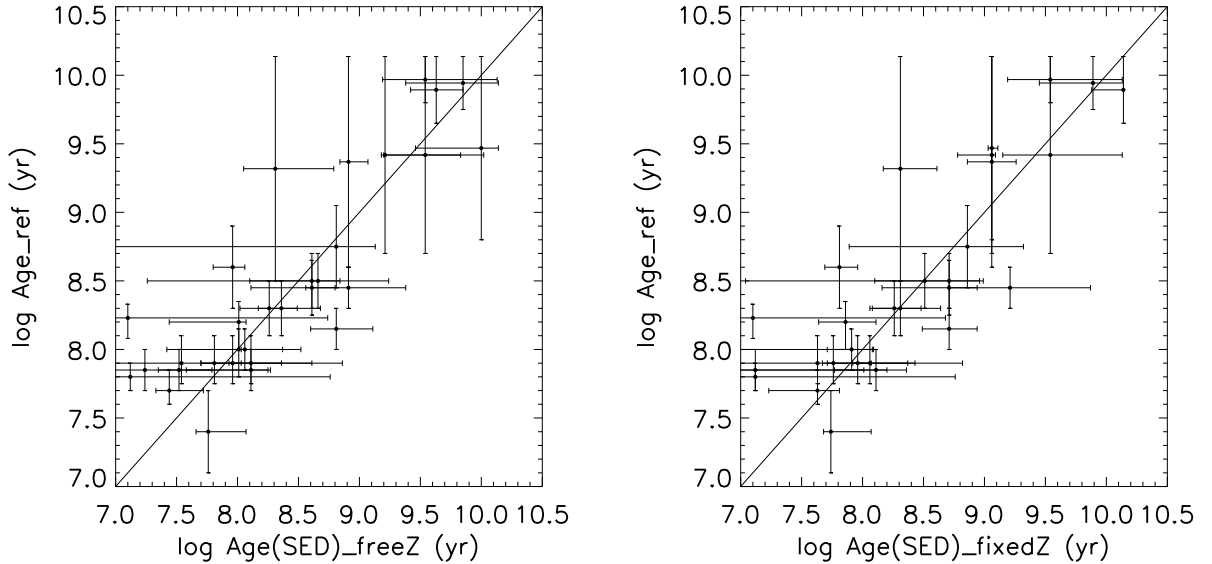


Fig. 2.— Same as Figure 1 but for the results fit with photometry without *FUV/NUV* bands, which significantly affect the age estimate for the BC03 models.

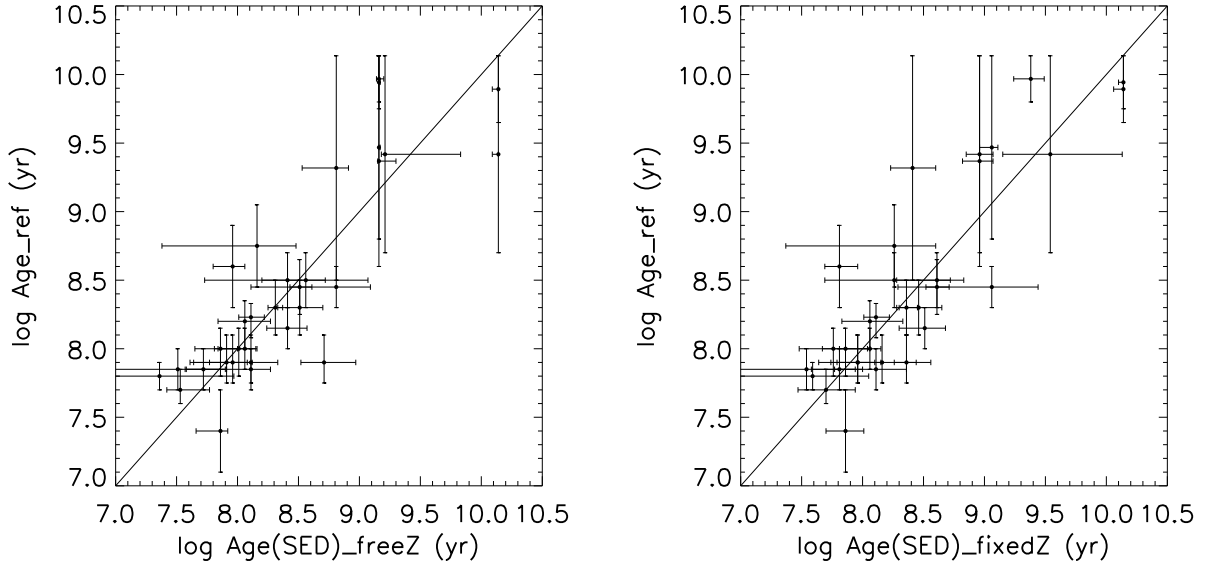


Fig. 3.— Same as Figure 2 but for the results fit without photometry only of WISE *W1*/*W2* bands, which seems dose not affect much for the age estimate for the BC03 models.

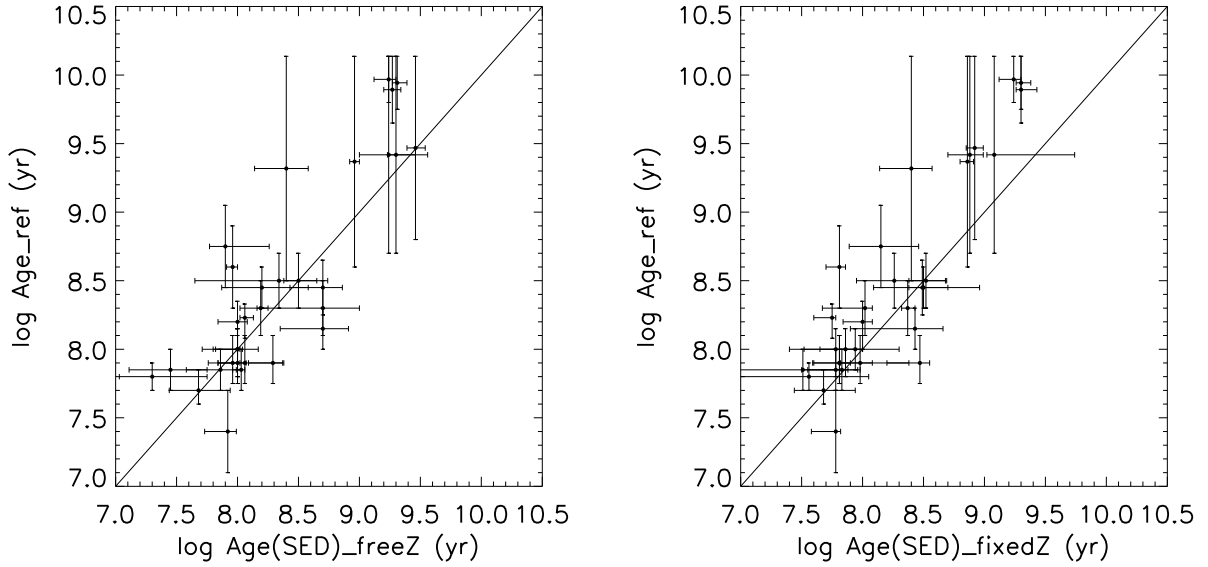


Fig. 4.— As Figure 1 but for *GALEV* models and a Kroupa (2001) IMF with all-band photometry.

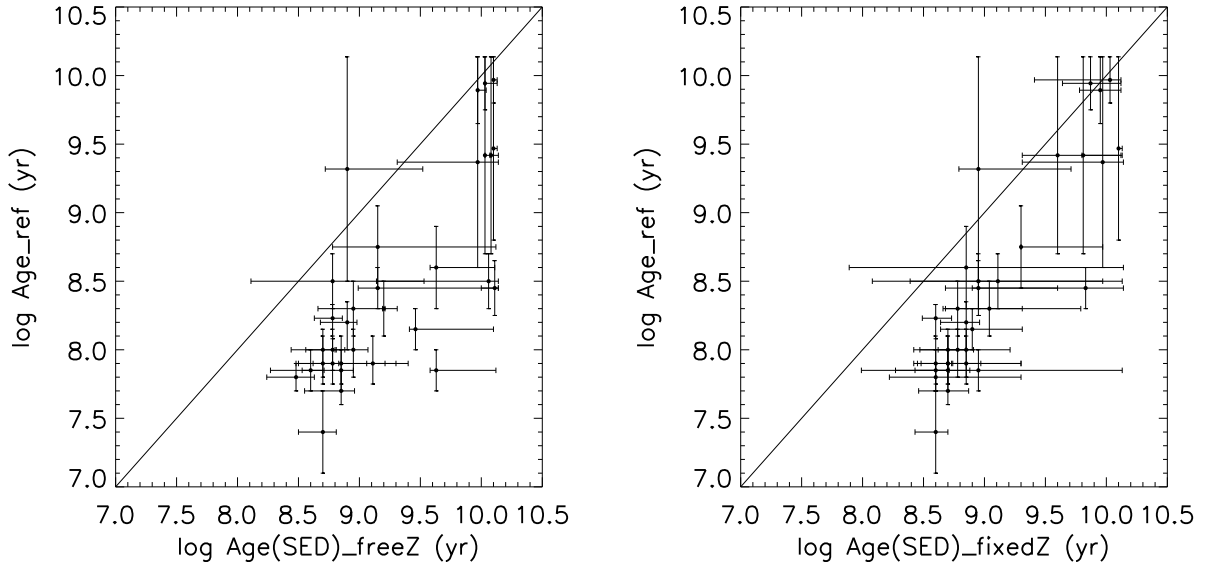


Fig. 5.— As Figure 1 but for the ASPS SSP models with all-band photometry without WISE W1/W2 band, which are not included in the model.

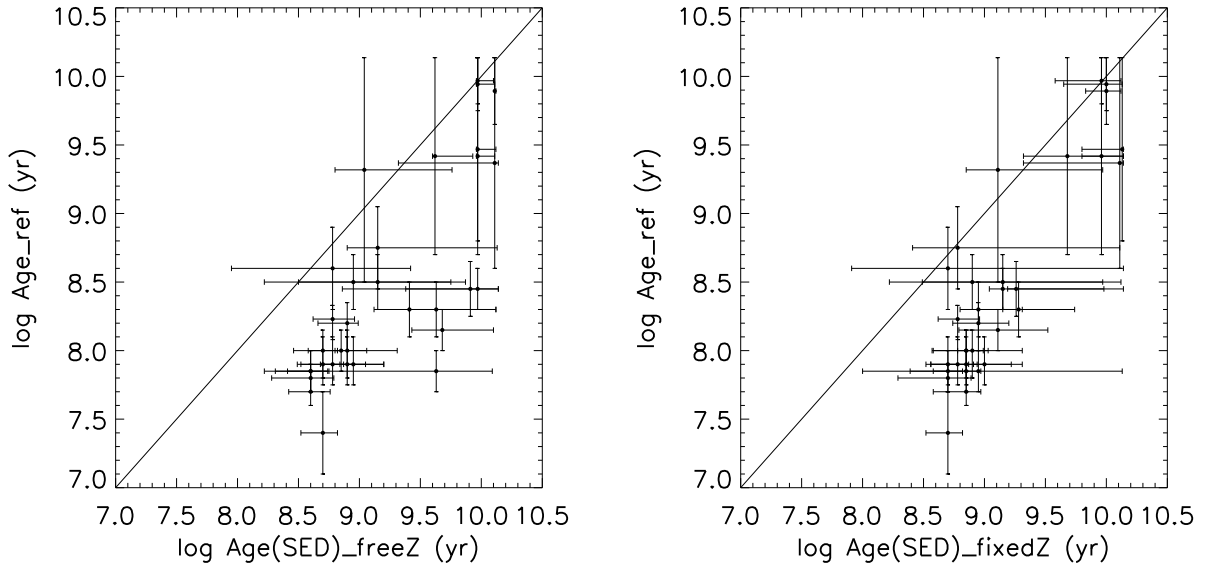


Fig. 6.— As Figure 1 but for the ASPS BSP models with all-band photometry without WISE W1/W2 band, which are not included in the model.

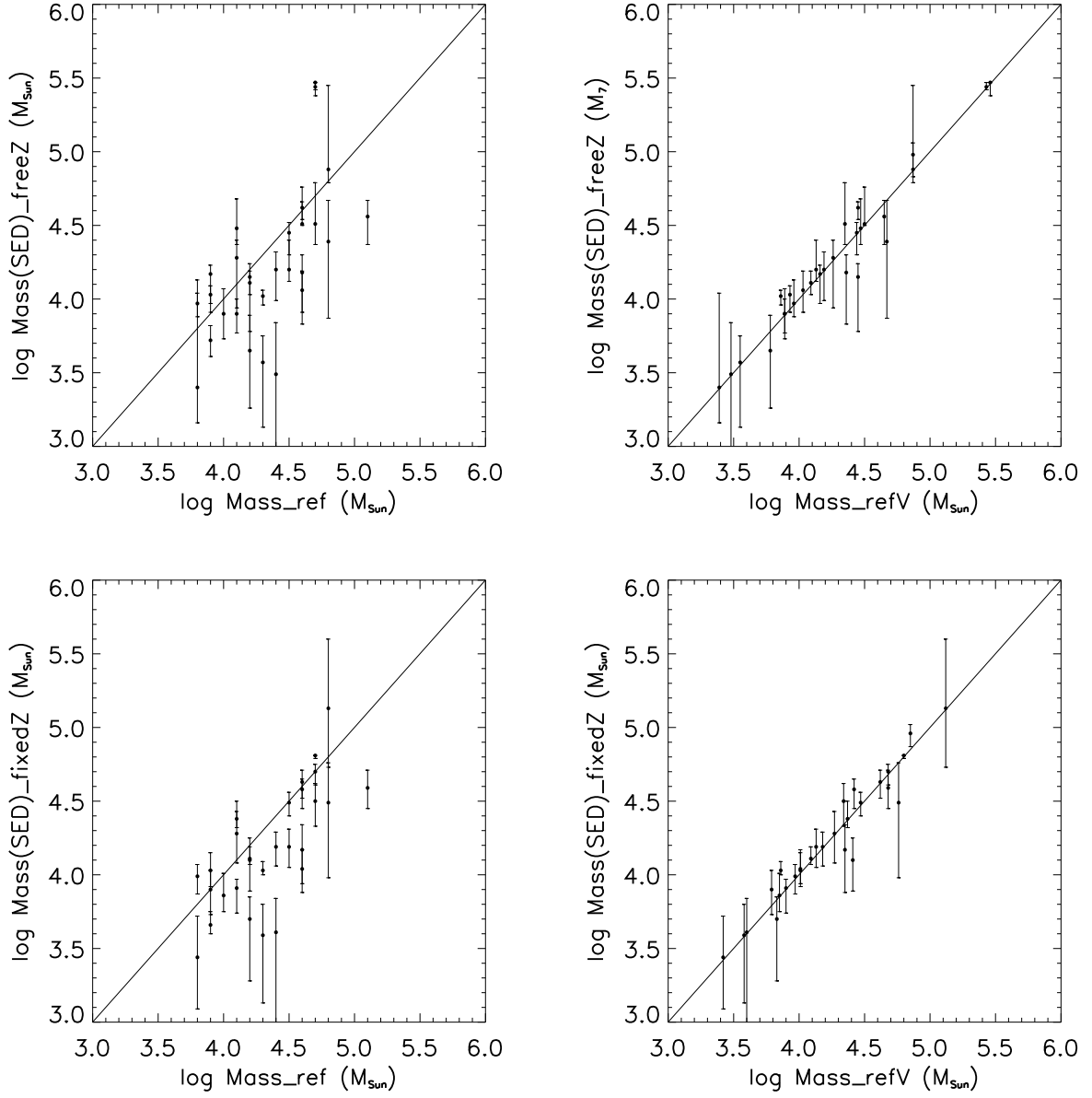


Fig. 7.— Mass comparisons resulting from fits employing the BC03 models using photometry with free-Z fit (top) and those with fixed-Z fit (bottom). Padova 2000 evolutionary tracks and a Chabrier (2003) IMF are adopted.

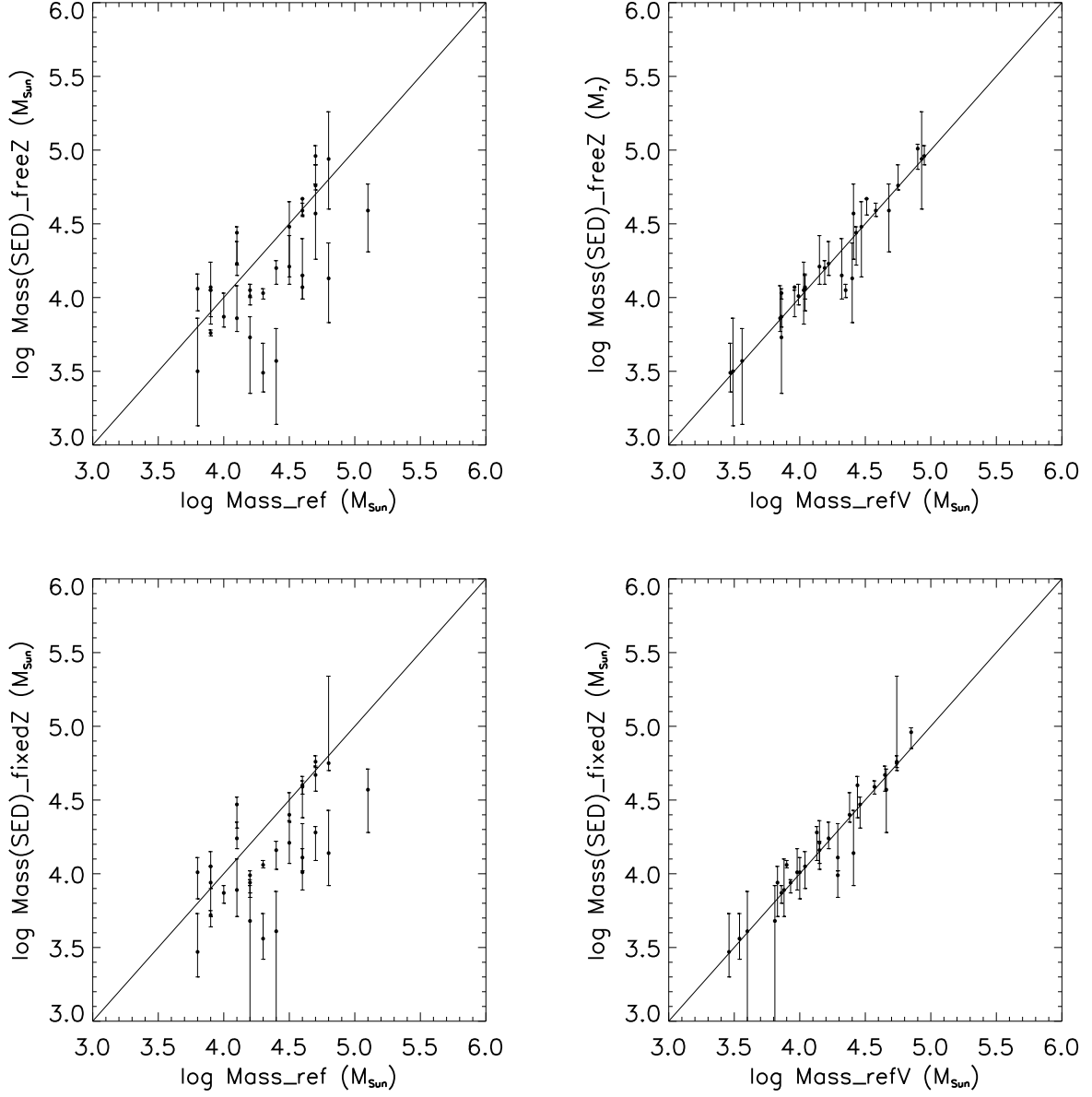


Fig. 8.— Same as Figure 7 but for *GALEV* models and Kroupa (2001) IMF using photometry with free-Z fit (top) and those with fixed-Z fit (bottom).

